Phosphatidyl Inositol 3-Kinase Signaling in Hypothalamic Proopiomelanocortin Neurons Contributes to the Regulation of Glucose Homeostasis

Jennifer W. Hill,[a] Yong Xu,[a] Frederic Preitner, Makota Fukuda, You-Ree Cho, Ji Luo, Nina Balthasar, Roberto Coppari, Lewis C. Cantley, Barbara B. Kahn, Jean J. Zhao,[b] and Joel K. Elmquist[b]

Division of Hypothalamic Research (J.W.H., Y.X., R.C., J.K.E.), Department of Internal Medicine and Pharmacology, Department of Internal Medicine and Cell Biology (Y.-R.C.), Touchstone Center for Diabetes Research, The University of Texas Southwestern Medical Center, Dallas, Texas 75390; Cardiomet Mouse Metabolic Facility (F.P.), Center for Integrative Genomics, University of Lausanne, CH-1015 Lausanne, Switzerland; Departments of Genetics (J.L.), Systems Biology (L.C.C.), and Pathology (J.J.Z.), Harvard Medical School, Department of Medicine (J.L.), Brigham and Women's Hospital, and Divisions of Signal Transduction (L.C.C.) and Endocrinology (B.B.K.), Beth Israel Deaconess Medical Center, and Department of Cancer Biology (J.J.Z.), Dana-Farber Cancer Institute, Boston, Massachusetts 02215; and Division of Physiology (N.B.), University of Bristol, Bristol BS8 1TD, United Kingdom

[a]J.W.H. and Y.X. are joint first authors.

[b]J.J.Z. and J.K.E. are joint senior authors.

Address all correspondence and requests for reprints to: Joel Elmquist, Division of Hypothalamic Research, Department of Internal Medicine, The University of Texas Southwestern Medical Center, 5323 Harry Hines Boulevard, Dallas, Texas 75390-9077. E-mail: joel.elmquist@utsouthwestern.edu ; or Jean Zhao, Dana-Farber Cancer Institute, 44 Binney Street, Smith 936B, Boston, Massachusetts 02115. E-mail: jean_zhao@dfci.harvard.edu .

Abstract

Recent studies demonstrated a role for hypothalamic insulin and leptin action in the regulation of glucose homeostasis. This regulation involves proopiomelanocortin (POMC) neurons because suppression of phosphatidyl inositol 3-kinase (PI3K) signaling in these neurons blunts the acute effects of insulin and leptin on POMC neuronal activity. In the current study, we investigated whether disruption of PI3K signaling in POMC neurons alters normal glucose homeostasis using mouse models designed to both increase and decrease PI3K-mediated signaling in these neurons. We found that deleting p85α alone induced resistance to diet-induced obesity. In contrast, deletion of the p110α catalytic subunit of PI3K led to increased weight gain and adipose tissue along with reduced energy expenditure. Independent of these effects, increased PI3K activity in POMC neurons improved insulin sensitivity, whereas decreased PI3K signaling resulted in impaired glucose regulation. These studies show that activity of the PI3K pathway in POMC neurons is involved in not only normal energy regulation but also glucose homeostasis.

Diabetes rates along with obesity are rising in the United States (1,2), causing substantial life span reductions (3,4,5). Recent studies implicate insulin and leptin in the central regulation of glucose homeostasis. Hypothalamic insulin signaling suppresses hepatic glucose production (HGP), which is elevated in type 2 diabetes (6,7,8). Likewise, central leptin alters peripheral glucose uptake and hepatic glucose output (9,10,11) and rescues hyperphagia-induced hepatic insulin resistance (12). Leptin-deficient mice have impaired insulin and glucose homeostasis (13) that is normalized by leptin administration (14). Furthermore, reexpressing leptin receptors in the arcuate nucleus of leptin receptor null mice reduces hyperglycemia (15,16,17).

Both insulin and leptin activate the phosphatidyl inositol 3-kinase (PI3K) intracellular signaling pathway (18). PI3K consists of an 85-kDa regulatory (p85) and a 110-kDa catalytic (p110) subunit (19), each having several isoforms. p85 binds insulin receptor substrate (IRS) molecules and localizes catalytic activity to the cell membrane, In which p110 phosphorylates phospatidylinositol 4,5-biphosphate (PIP2) to phosphatidylinositol-3,4,5-trisphosphate (PIP3), activating downstream molecules that bind PIP3 such as Akt. Reduced gene dosage of the catalytic subunit, as occurs in p110α inactivated cells or tissues, causes a severe reduction in insulin-stimulated PI3K activity, pAkt, and the phosphorylation levels of downstream components such as Forkhead box O-transcription factors (20,21). However, genetic inactivation of the regulatory subunit paradoxically increases signaling downstream of PI3K (22). This increase seems to result from both a compensatory increase in p85β expression (23) and reduced phosphatase and tensin homolog deleted from chromosome 10 (PTEN) activity because p85α forms part of the PTEN-activating complex (24). PTEN dephosphorylates PIP3, antagonizing the action of PI3K. Therefore, the loss of p85-induced Akt activation is due, in part, to decreased PTEN activity protecting the PIP3 pool produced by the remaining p110-p85β heterodimers.

Hypothalamic proopiomelanocortin (POMC) neurons are essential for normal body weight homeostasis (25,26,27,28,29) and may be important for glucose homeostasis as well. Centrally administered melanocortin agonists inhibit insulin release and alter glucose uptake and production (10). Furthermore, POMC-specific deletion of suppressor of cytokine signaling (SOCS)-3, a negative regulator of both leptin and insulin signaling, results in improved glucose homeostasis and insulin sensitivity (30). We recently showed that deleting both p85α and p85β from POMC neurons eliminates insulin and leptin effects on POMC neuronal activity (31). We therefore investigated whether normal glucose homeostasis requires POMC PI3K signaling using mouse models designed to either increase or decrease PI3K activity in these neurons. Using the cre/loxP system, we investigated mice lacking p85α in POMC neurons (up-regulation of PI3K mediated signaling) and mice lacking p110α in POMC neurons (down-regulation of PI3K mediated signaling).

Materials and Methods

Animal care

Care of all animals and procedures was approved by the University of Texas Southwestern Medical Center (*pik3CA POMCKO* studies) and the Beth Israel Deaconess Medical Center (*pik3r1 POMCKO* studies) Institutional Animal Care and Use Committees. Mice were housed in a temperature-controlled environment in groups of two to four at 22–24 C using a 14-h light, 10-h dark cycle. The mice were fed either standard chow (4% fat mouse/rat diet 7001; Harlan-Teklad, Madison, WI) or high-fat diet (88137 Western diet; Harlan Teklad), and water was provided *ad libitum* unless noted otherwise. Mice were killed by CO_2 narcosis.

Generation of mouse lines

Pomc-Cre mice [FVB background (26)] were mated with *pik3r1^{loxP/loxP}* mice [129/Sv-C57BL/6-FVB mixed background (32)] or *pik3CA ^{loxP/loxP}* mice [129/SvJ-C57BL/6 mixed background (21)]. Breeding colonies were maintained by mating *pik3r1^{loxP/loxP}* mice with *pik3r1 POMCKO* mice and *pik3CA ^{loxP/loxP}* with *pik3CA POMCKO* mice. Thus, littermate controls with the same genetic background as experimental animals except for POMC-cre expression were used for all experiments. Any mouse that tested positive for deletion of the *pik3r1* or *pik3CA* gene in tail tissue was excluded from all studies. Genotyping was performed according to protocols described previously (21,31).

Immunohistochemistry and *in situ* hybridization

Fed male 10-wk-old mice were perfused with 10% neutral buffered formalin (Sigma-Aldrich, St. Louis, MO), and frozen coronal sections were cut at 25 μm (1:5 series) on a microtome. Sections were processed as reported previously from our laboratory (33).

To create the p85α and p110α cRNA probes (34), we used RT-PCR amplification. The first-strand cDNA was obtained using total rat brain RNA (Ambion, Inc., Austin, TX) as a template. For the p85α probe, the cDNA was then amplified by PCR using the 5′ primer: 5′-AGA ACG GCT ATC GAA GCA-3′ corresponding to nt 1997-2015 and the 3′ primer: 5′-GAC GCA ATG CTT GAC TTC-3′corresponding to nt 2552-2569 of p85α. The region bounded by these primers is 572 bases and corresponds to the COOH-terminal Src homology 2 domain of p85α. For the p110α probe, the cDNA was then amplified by PCR using the 5′ primer: 5′-TGC GCT GGG TAC TGC GTG GC-3′ corresponding to nt 2701-2720 and the 3′ primer: 5′-TAC GTT CAA AGC ATG CT-3′corresponding to nt 3191-3207 of p110α. The region bounded by these primers is 506 bases. The amplification products were gel purified and cloned into pCR4-TOPO vector (Invitrogen, Carlsbad, CA), by using standard techniques according to the manufacturer's protocol. The inserts of positive clones were verified by DNA sequencing with primers specific to the vector, T7 Sequenase (Amersham Life Science, Inc., Arlington Heights, IL), and the [35]Sequetide system from NEN Life Science Products (Boston, MA). To generate antisense ^{35}S-labeled cRNA, the plasmids were linearized by digestion with *Pst*I (p85α) or *Not*I (p110α) and subjected to *in vitro* transcription with T7 (p85α) or T3 (p110α) RNA polymerase according to the manufacturer's protocol (Promega, Madison, WI). For generation of sense ^{35}S-labeled cRNA, the plasmids were linearized by digestion with *Not*I (p85α) or *Pme*I (p110α) and subjected to *in vitro* transcription with T3 (p85α) or T7 (P110α) RNA polymerase according to the manufacturer's protocol.

The ^{35}S-labeled probes were diluted to 10^6 cpm/ml and used for *in situ* hybridization as previously described (33). Where applicable, after free-floating *in situ* hybridization histochemistry (ISHH), tissue was stained with a β-endorphin antibody (H-022-33; Phoenix Pharmaceuticals, Burlingame, CA) following established protocols. Tissue was mounted on slides for exposure to film and analysis by microscope. Very stringent criteria were used to assess coexpression to minimize false positives; coexpression was considered present if silver grains clustered around the outline of the cell beneath.

Feeding studies and body composition

Mice were housed individually for all body weight and food intake measurements. Body weight and chow consumption were measured once every 7 d. Food pellets were replaced weekly to reduce spillage. Body composition was determined using quantitative magnetic resonance (Minispec MQ10; Bruker, Houston, TX) for the *pik3CA POMCKO* mice by dual-energy x-ray absorptiometry (DEXA) for the *pik3r1 POMCKO* mice and controls. Mice were ketamine anesthetized for DEXA (MEC Lunar Corp., Minster, OH) using the facilities of the Metabolic Physiology Core of the Diabetes Endocrinology Research Center at Beth Israel Deaconess Medical Center.

Hormone measurements

For leptin and insulin assays, tail vein blood was obtained from *ad libitum* chow-fed mice at 12 wk of age unless otherwise specified. Serum was collected by centrifugation and assayed by commercially available ELISA kits (Crystal Chem Inc., Downers Grove, IL).

Corticosterone concentrations were measured from tail vein blood collected 30 min after an ip glucose injection (2 g/kg) to mimic experimental conditions in which differing corticosterone levels might alter glucose levels. Serum was measured by ELISA (correlate-EIA corticosterone kit; Assay Designs, Ann Arbor, MI) according to the manufacturer's instructions.

Evaluation of glucose homeostasis

Glucose in tail blood was assayed using a glucometer (One-Touch Basic; Lifescan, Milpitas, CA), with postprandial measurements taken at approximately 1000 h. Where indicated, blood was obtained from mice fasted for 16 h. For insulin tolerance tests, 3 h-fasted animals were injected ip with 1 mU/g human insulin (Humulin R; Eli Lilly Corp., Indianapolis, IN), and blood glucose values were measured immediately before and 15, 30, 45, 60, 90, and 120 min after injection. For glucose tolerance tests, overnight-fasted mice were injected with D-glucose (1 mg/g body weight), and blood glucose was measured immediately before and 15, 30, 45, 60, and 120 min after injection. Study mice (12–16 wk of age) were maintained on chow and matched for body weight and adiposity for analysis.

Metabolic chambers

Locomotor activity, respiratory quotients, and oxygen consumption were measured in *pik3r1 POMCKO* mice in a Columbus Instruments CLAMS by the Beth Israel Deaconess Medical Center Animal Physiology Core as previously described (15). Physical activity, energy expenditure, and heat production were monitored in *pik3CA POMCKO* mice using a combined indirect calorimetry system (TSE Systems GmbH, Bad Homburg, Germany) (35). For the latter, mice were housed individually at room temperature (22 C) under an alternating 12-h light, 12-h dark cycle. After adaptation for 6 d, home-cage physical activity was determined for 4 d using a multidimensional infrared light beam system with beams installed on cage bottom and cage top levels. Ambulatory movement was defined as breaks of any two different light beams at cage bottom level. Simultaneously O_2 consumption, CO_2 production, and heat production were measured to determine energy expenditure. In addition, food intake was determined continuously.

Hyperinsulinemic euglycemic clamps

At 3–5 d before clamp experiments, mice were anesthetized, and a silicone catheter was inserted in the femoral vein as previously described (36) and externalized through skin at the nape of the neck. The catheter was flushed daily with sterile saline until the animal returned to its preoperative weight. Mice were then fasted for 16 h and then subjected to a 120-min basal clamp followed by a 120-min hyperinsulinemic-euglycemic clamp study in an awake and unrestrained state. During 2 h of basal clamping, the animals were infused with (3-^{3}H) glucose solution (6 μCi total at a rate of 0.05 μCi per 3.3 μl/min) to measure HGP. Blood (30 ml) was sampled from the tail vein 5 min before the end of this period. Then mice received a prime dose of insulin (Humulin R, regular human insulin; Lilly) followed by a continuous infusion of insulin (15 pmol/kg body weight) at a rate of 3 μl/min. A 40% glucose solution was also infused at variable rates and periodically adjusted to maintain the plasma glucose levels at about 6.5 mM. The plasma glucose level was monitored using a glucometer every 10 min (5 ml). A (3-^{3}H) glucose solution was infused through the jugular vein catheter (10 μCi bolus, followed by 0.1 μCi/3 μl/min). Forty-five minutes before the end of study, a bolus of 2-deoxy-D-(1-^{14}C) glucose [2-(^{14}C) DG] was injected through the catheter to estimate insulin-induced glucose uptake in individual tissues (10 μCi per 10 μl). Blood was collected from the tail vein (25 μl at 5, 15, 25, 35, and 45 min after the deoxyglucose injection) to estimate whole-body glucose flux and the disappearance curve of the 2-(^{14}C) DG from blood. After termination of the experiment, white adipose and brown adipose tissues, heart, skeletal muscle, liver, and brain were collected, and 2-(^{14}C) DG content in the tissues was measured.

Western blot analysis

Samples were obtained from the liver 10 min after a 5 U/kg ip injection of insulin and immediately frozen on dry ice. Whole-cell protein extraction was performed. Equal amounts of the samples were separated by SDS-PAGE and visualized after electrophoretical transfer via binding of specific primary and horseradish peroxidase-conjugated secondary antibodies followed by chemiluminescent detection using West Pico chemiluminescent substrate (Thermo Fisher Scientific Inc., Waltham, MA). The primary

antibodies were a 1:1,000 dilution of the antibody against phospho-Akt (serine-473; Cell Signaling Technology, Beverly, MA), and a 1:10,000 dilution of the antibody against β-actin (Santa Cruz Biotechnology, Santa Cruz, CA).

Statistics

The data are reported as mean ± SEM. Comparisons between two groups were made by unpaired two-tailed t tests. Comparisons over time were carried out by calculating area under the curve for blood glucose levels or by repeated-measure ANOVA for body weight curves. $P < 0.05$ was considered to be statistically significant. All statistical analyses were performed using Prism software (version 5.0; GraphPad Software, San Diego, CA).

Results

Previous studies have shown that ablation of *pik3r1*, the gene encoding p85α, leads to increased PIP3 levels and subsequent activation of signaling pathways downstream of PI3K (22,23,37,38,39). To generate mice with increased PI3K signaling in POMC neurons, we crossed mice carrying a floxed allele of *pik3r1* gene (40) with transgenic mice expressing Cre-recombinase driven by *Pomc* regulatory elements (26) to create *pik3r1 POMCKO* mice. To generate a second group of mice with reduced PI3K signaling in POMC neurons, we crossed mice carrying a floxed allele of the *pik3CA* gene encoding p110α (21) with *Pomc*-Cre transgenic mice to create *pik3CA POMCKO* mice. For all experiments, mice were compared with littermates not expressing POMC-cre (*pik3r1[loxP/loxP]* or *pik3CA[loxP/loxP]* mice).

Using ISHH, we first examined arcuate nucleus expression of pik3r1 and pik3ca. We found that both genes have extensive expression throughout the arcuate nucleus with a characteristic pattern of hypothalamic mRNA localization (Fig. 1, A and B). We previously demonstrated that deletion of the loxP-flanked region of *pik3r1* in the brains of *pik3CA POMCKO* mice is limited to POMC-expressing areas (31). Likewise, deletion of the loxP-flanked region of pik3CA was restricted to expected regions (supplemental Fig. S1A published on The Endocrine Society's Journals Online web site at http://endo.endojournals.org). A subsequent immunohistochemistry analysis of β-endorphin in these POMC neurons revealed that p85α and p110α are expressed in POMC neurons (Fig. 1, C and D). In *pik3r1 POMCKO* or *pik3CA POMCKO* mice, POMC mediated Cre expression efficiently ablated *pik3r1* or *pik3ca* in POMC neurons (Fig. 1, C and D and supplemental Fig. S1B).

We next examined body weight changes on normal chow in males and females of all genotypes. Mice with POMC neuron-specific ablation of p110α displayed a modest increase in body weight. (Fig. 2, A and B). No change was seen in body length (data not shown). To examine the mechanism underlying the weight gain in *pik3CA POMCKO* mice, we placed weight-matched cohorts of *pik3CA POMCKO* and their littermate controls in metabolic chambers. Whereas no change was observed in food intake or activity levels in these mice (Fig. 2, C and D), female *pik3CA POMCKO* mice had significantly lower energy expenditures than weight- and gender-matched controls, as measured by decreased O_2 consumption as well as reduced heat production (Fig. 2, E and G). No difference was seen in the mass of brown adipose tissue from *pik3CA POMCKO* mice (68.17 mg ± 5.07 controls *vs.* 62.67 mg ± 6.87 *pik3CA POMCKO*). The respiratory exchange ratio did not differ between groups arguing against any change in preference for carbohydrate or lipid as substrates. (Fig. 2F). These results suggest that decreased energy expenditure, at least in females, contributes to the increased body weight of *pik3CA POMCKO* mice.

We next examined whether susceptibility to diet-induced obesity changed in mice with altered PI3K signaling in POMC neurons. We found that *pik3r1 POMCKO* females failed to gain weight on high-fat chow to the same extent as their littermate controls (Fig. 3B). In addition, these females exhibited significantly lower fat mass and leptin levels than control mice (Fig. 3, D and H). Conversely, *pik3CA POMCKO* mice showed increased body weight on high-fat chow accompanied by an increased fat mass (Fig. 3, A–D).

As previously mentioned, POMC neurons have been shown to regulate glucose homeostasis (10,30). We therefore went on to examine the effects of altered PI3K activity in POMC neurons on glucose homeostasis in mice with POMC-specific loss of p85α or p110α. Because glucocorticoids can cause glucose intolerance and insulin resistance (41,42,43), we first looked for evidence of changes in the hypothalamus-pituitary-adrenal axis downstream of POMC-expressing corticotrophs by examining corticosterone production under experimental conditions (described in *Materials and Methods*). We found that levels of corticosterone did not differ between the experimental animals and littermate controls (Fig. 4A). These results are in agreement with our previous findings of normal corticosterone production in mice lacking both *pik3r1* and *pik3r2* in POMC neurons (31).

We next examined basal glucose and insulin levels in chow-fed male mice. All measurements of glucose homeostasis were made in chow-fed body weight-matched and fat mass-matched mice to avoid the confounding effects of differing adiposity levels between mutant mice and littermate controls. Male *pik3r1 POMCKO* mice exhibited lower basal insulin levels with no obvious changes in glucose levels, suggesting that ablation of p85α in POMC neurons increased insulin sensitivity (Fig. 4, B and C). In contrast, *pik3CA POMCKO* mice showed both elevated insulin and glucose levels, indicating that POMC neuron-specific loss of p110α resulted in impaired insulin sensitivity. However, no evidence of glucose intolerance was seen in *pik3r1 POMCKO* mice or *pik3CA POMCKO* mice in response to a glucose bolus (Fig. 4D). We then subjected mice of all genotypes to an insulin tolerance test. The *pik3CA POMCKO* mice showed a significant impairment in blood glucose suppression in response to insulin stimulation (Fig. 4E). To investigate whether altered PI3K signaling in POMC neurons affects liver insulin sensitivity, we examined Akt activation in liver tissue taken 10 min after a bolus of insulin (5 U/kg). Akt phosphorylation was clearly reduced in tissue from *pik3CA POMCKO* mice (Fig. 5A); however, a change in pAkt levels could not be clearly shown in *pik3r1 POMCKO* hepatic tissue (data not shown).

For a more sensitive measure of hepatic and peripheral insulin sensitivity of *pik3r1 POMCKO* mice, we subjected them to hyperinsulinemic, euglycemic clamps. Basal HGP was significantly decreased in *pik3r1 POMCKO* mice (Fig. 5A). Given that during the basal period endogenous insulin acts chiefly on liver rather than muscle, this result suggests increased hepatic insulin sensitivity in these mice. In the hyperinsulinemic state, the glucose infusion rate tended to be higher in *pik3r1 POMCKO* mice, although the values did not reach statistical significance (Fig. 5B). However, the extent of suppression of HGP was significantly greater than controls in response to a fixed elevated insulin level (Fig. 5C). We went on to investigate hepatic insulin sensitivity under basal and clamp steady-state conditions by measuring expression levels of protein tyrosine phosphatase-1B (PTP1B). PTP1B dephosphorylates the insulin receptor and blunts its ability to transduce signal, thus mediating insulin resistance (44). We found that the expression of PTP1B was significantly suppressed in *pik3r1 POMCKO* hepatic tissue after hyperinsulinemic clamping (Fig. 5F), suggesting that loss of p85α in POMC neurons improved insulin sensitivity in the liver. Taken together, these data suggest that PI3K activity in POMC neurons can suppress glucose production by the liver and support the model that PI3K signaling in POMC neurons indirectly regulates hepatic insulin signaling.

Discussion

Recent studies suggest that insulin acting on central pathways can exert a potent effect on peripheral glucose metabolism, including HGP (8,10). In addition, leptin may play a critical role in glucose homeostasis, as restoration of leptin receptors to the arcuate nucleus or transgenic overexpression of the POMC gene reduces hyperglycemia in leptin receptor null animals (15,45). Thus, we hypothesized that PI3K signaling in POMC neurons is involved in whole-body glucose homeostasis.

Taking advantage of the specialized roles of the PI3K regulatory and catalytic subunits, we now used targeted deletion of p85α or p110α to selectively up-regulate or down-regulate PI3K-mediated activity,

respectively, in POMC neurons. We found that although both groups maintained glucose tolerance, *pik3r1 POMCKO* displayed an increase in insulin sensitivity, and *pikCA POMCKO* mice displayed a decrease in insulin sensitivity as determined by basal insulin levels, insulin tolerance testing, and/or hyperinsulinemic euglycemic clamping.

Previous studies using targeted perturbation in POMC neurons largely supported a role for POMC PI3K signaling in glucose homeostasis, although definitive evidence has been lacking. Mice lacking 3-phosphoinositide-dependent protein kinase-1, an enzyme downstream of PI3K, in POMC neurons initially displayed impaired glucose metabolism (46). However, these results were confounded by severe hypocortisolism caused by loss of POMC-expressing corticotrophs in the pituitary. In addition, selective deletion of SOCS-3, a negative regulator of leptin and insulin signaling, in POMC neurons led to a significant improvement in glucose homeostasis and insulin sensitivity without any apparent impact on the adrenal axis (30). However, mice lacking insulin receptors in POMC neurons did not show any defect in glucose or energy homeostasis (47). Mice with POMC-specific disruption of PTEN, expected to result in constitutively high levels of PI3K signaling, were apparently not evaluated for insulin levels or glucose regulation (48). We previously examined the effect of simultaneous deletion of both regulatory subunits, p85α and p85β, from POMC neurons by crossing *pik3r1 POMCKO* mice with mice germline knockout for pik3r2 (31). We found that concurrent loss of these two p85 subunits in POMC neurons abolishes the ability of these neurons to respond to leptin or insulin stimulation, but any effect on glucose homeostasis could not be evaluated due to increased insulin sensitivity in the global p85β-null mice. Our current data establish that alteration of PI3K activity in POMC neurons can modulate hepatic insulin sensitivity and glucose regulation, providing a mechanistic link between the response of POMC neurons to leptin or insulin and their effects on glucose homeostasis (30,45).

In the current experiments, we also observed an effect of POMC neuronal PI3K activity on body weight regulation. This finding extends our prior study of the effect of PI3K regulatory subunits on body weight (30). Whereas ablation of both p85α and p85β subunits in POMC neurons was required to impair POMC neuronal activity in response to insulin and leptin as well as acute leptin-induced feeding, no obvious impact on long-term body weight regulation was observed in those mice (31). The contrast to the current results may arise from the fact that global deletion of p85β has been reported to reduce mouse size and affect insulin sensitivity (49). Thus, it is possible that the experimental animals were protected from developing obesity in the initial study. This interpretation is in agreement with results from mice lacking SOCS-3 in POMC neurons showing reduction in weight gain on a high-fat diet (30). In addition, Plum *et al.* (48) have shown that POMC-specific disruption of PTEN results in hyperphagia, male obesity on normal chow, and female obesity on high-fat chow. However, interpretation of the latter results is complicated by morphological changes in POMC neurons and the existence of other downstream targets of PTEN, including MAPK and Shc (50,51,52,53,54).

Our results show that deletion of a single p85 isoform results in resistance to diet-induced obesity in female mice, possibly because the well-known anorexigenic effects of estrogens may be enhanced through increased PI3K signaling in POMC neurons (55,56,57). In addition, mice with increased PI3K activity in POMC neurons diverged from control values over time, whereas the body weight of mice with reduced PI3K signaling in these neurons tended to converge with control values. This observation is consistent with the hypothesis that high-fat feeding promotes weight gain in part by reducing PI3K signaling in POMC neurons.

These studies focused on the actions of the p110α catalytic subunit, although a p110β isoform also exists in the brain (58,59,60). p110α is selectively recruited and activated by the IRS signaling complex and is required for leptin and insulin-induced IRS-1/2-associated PI3K activity in the hypothalamus (20,61). Mice heterozygous for a kinase-inactive p110α mutation display hyperinsulinemia, glucose intolerance, hyperphagia, and increased adiposity without compensatory up-regulation of the activity of p110β (20).

In contrast, p110β does not appear to play a significant role in insulin-stimulated Akt activation (61,62), although interesting kinase-independent actions have recently been demonstrated in liver (67). Thus, it would be intriguing to examine the metabolic and glucoregulatory impact of p110β deletion as well.

In conclusion, these studies demonstrate that the PI3K pathway in POMC neurons plays a role in hepatic insulin sensitivity and glucose homeostasis. Moreover, PI3K signaling in POMC neurons has the ability to influence body weight regulation, especially in response to a high-fat dietary challenge.

Supplementary Material
[Supplemental Data]

Acknowledgments

We thank Michelle Choi, Charlotte Lee, Frank Marino, Brad Lampe, Sarah Greeley, Damalie Namponye, and the Mouse Metabolic Phenotyping Core at University of Texas Southwestern Medical Center at Dallas (supported by Grant PL1 DK081182-01) for assistance in performing studies described in this paper.

Footnotes

Disclosure Summary: The authors have nothing to declare.

First Published Online October 9, 2009

Abbreviations: 2-(^{14}C) DG, 2-Deoxy-D-(1-^{14}C) glucose; DEXA, dual-energy x-ray absorptiometry; HGP, hepatic glucose production; IRS, insulin receptor substrate; ISHH, *in situ* hybridization histochemistry; p85, 85-kDa regulatory subunit; p110, 110-kDa catalytic subunit; PI3K, phosphatidyl inositol 3-kinase; PIP3, phosphatidylinositol-3,4,5-trisphosphate; POMC, proopiomelanocortin; PTEN, phosphatase and tensin homolog deleted from chromosome 10; PTP1B, protein tyrosine phosphatase-1B; SOCS, suppressor of cytokine signaling.

References

1. **Flegal KM, Carroll MD, Ogden CL, Johnson CL**2002 Prevalence and trends in obesity among U.S. adults, 1999–2000. JAMA 288:1723–1727.
2. **Kuczmarski RJ, Flegal KM, Campbell SM, Johnson CL**1994 Increasing prevalence of overweight among U.S. adults. The National Health and Nutrition Examination Surveys, 1960 to 1991. JAMA 272:205–211.
3. **Allison DB, Fontaine KR, Manson JE, Stevens J, VanItallie TB**1999 Annual deaths attributable to obesity in the United States. JAMA 282:1530–1538.
4. **Fontaine KR, Redden DT, Wang C, Westfall AO, Allison DB**2003 Years of life lost due to obesity. JAMA 289:187–193.
5. **Manuel DG, Schultz SE**2004 Health-related quality of life and health-adjusted life expectancy of people with diabetes in Ontario, Canada, 1996–1997. Diabetes Care 27:407–414.
6. **Gelling RW, Morton GJ, Morrison CD, Niswender KD, Myers Jr MG, Rhodes CJ, Schwartz MW**2006 Insulin action in the brain contributes to glucose lowering during insulin treatment of diabetes. Cell Metab 3:67–73.
7. **Inoue H, Ogawa W, Asakawa A, Okamoto Y, Nishizawa A, Matsumoto M, Teshigawara K, Matsuki Y, Watanabe E, Hiramatsu R, Notohara K, Katayose K,**

Okamura H, Kahn CR, Noda T, Takeda K, Akira S, Inui A, Kasuga M2006 Role of hepatic STAT3 in brain-insulin action on hepatic glucose production. Cell Metab 3:267–275.

8. **Obici S, Zhang BB, Karkanias G, Rossetti L**2002 Hypothalamic insulin signaling is required for inhibition of glucose production. Nat Med 8:1376–1382.

9. **Lin CY, Higginbotham DA, Judd RL, White BD**2002 Central leptin increases insulin sensitivity in streptozotocin-induced diabetic rats. Am J Physiol Endocrinol Metab 282:E1084–E1091.

10. **Obici S, Feng Z, Tan J, Liu L, Karkanias G, Rossetti L**2001 Central melanocortin receptors regulate insulin action. J Clin Invest 108:1079–1085. [PMCID: PMC200952]

11. **Rossetti L, Massillon D, Barzilai N, Vuguin P, Chen W, Hawkins M, Wu J, Wang J** 1997 Short term effects of leptin on hepatic gluconeogenesis and *in vivo*insulin action. J Biol Chem 272:27758–27763.

12. **Pocai A, Lam TK, Gutierrez-Juarez R, Obici S, Schwartz GJ, Bryan J, Aguilar-Bryan L, Rossetti L**2005 Hypothalamic K(ATP) channels control hepatic glucose production. Nature 434:1026–1031.

13. **Coleman DL**1978 Obese and diabetes: two mutant genes causing diabetes-obesity syndromes in mice. Diabetologia 14:141–148.

14. **Pelleymounter MA, Cullen MJ, Baker MB, Hecht R, Winters D, Boone T, Collins F**1995 Effects of the obese gene product on body weight regulation in ob/ob mice. Science 269:540–543.

15. **Coppari R, Ichinose M, Lee CE, Pullen AE, Kenny CD, McGovern RA, Tang V, Liu SM, Ludwig T, Chua Jr SC, Lowell BB, Elmquist JK**2005 The hypothalamic arcuate nucleus: a key site for mediating leptin's effects on glucose homeostasis and locomotor activity. Cell Metabolism 1:63–72.

16. **Morton GJ, Niswender KD, Rhodes CJ, Myers Jr MG, Blevins JE, Baskin DG, Schwartz MW**2003 Arcuate nucleus-specific leptin receptor gene therapy attenuates the obesity phenotype of Koletsky [fa(k)/fa(k)] rats. Endocrinology 144:2016–2024.

17. **Morton GJ, Gelling RW, Niswender KD, Morrison CD, Rhodes CJ, Schwartz MW**2005 Leptin regulates insulin sensitivity via phosphatidylinositol-3-OH kinase signaling in mediobasal hypothalamic neurons. Cell Metab 2:411–420.

18. **Niswender KD, Baskin DG, Schwartz MW**2004 Insulin and its evolving partnership with leptin in the hypothalamic control of energy homeostasis. Trends Endocrinol Metab 15:362–369.

19. **Cantley LC**2002 The phosphoinositide 3-kinase pathway. Science 296:1655–1657.

20. **Foukas LC, Claret M, Pearce W, Okkenhaug K, Meek S, Peskett E, Sancho S, Smith AJ, Withers DJ, Vanhaesebroeck B**2006 Critical role for the p110α phosphoinositide-3-OH kinase in growth and metabolic regulation. Nature 441:366–370.

21. **Zhao JJ, Cheng H, Jia S, Wang L, Gjoerup OV, Mikami A, Roberts TM**2006 The p110α isoform of PI3K is essential for proper growth factor signaling and oncogenic transformation. Proc Natl Acad Sci USA 103:16296–16300. [PMCID: PMC1637576]

22. **Taniguchi C, Tran TT, Kondo T, Luo J, Ueki K, Cantley LC, Kahn CR**2006 Phosphoinositide 3-kinase regulatory subunit p85α suppresses insulin action via positive regulation of PTEN. Proc Natl Acad Sci USA 103:12093–12097. [PMCID: PMC1524929]

23. **Fruman DA, Mauvais-Jarvis F, Pollard DA, Yballe CM, Brazil D, Bronson RT, Kahn CR, Cantley LC**2000 Hypoglycaemia, liver necrosis and perinatal death in mice lacking all isoforms of phosphoinositide 3-kinase p85α. Nat Genet 26:379–382.

24. **Kotelevets L, van Hengel J, Bruyneel E, Mareel M, van Roy F, Chastre E**2005 Implication of the MAGI-1b/PTEN signalosome in stabilization of adherens junctions and suppression of invasiveness. FASEB J 19:115–117.

25. **Balthasar N**2006 Genetic dissection of neuronal pathways controlling energy homeostasis. Obesity (Silver Spring) 14(Suppl 5):222S–227S.

26. **Balthasar N, Coppari R, McMinn J, Liu SM, Lee CE, Tang V, Kenny CD, McGovern RA, Chua Jr SC, Elmquist JK, Lowell BB**2004 Leptin receptor signaling in POMC neurons is required for normal body weight homeostasis. Neuron 42:983–991.

27. **Butler AA**2006 The melanocortin system and energy balance. Peptides 27:281–290. [PMCID: PMC2735083]

28. **Coll AP**2007 Effects of pro-opiomelanocortin (POMC) on food intake and body weight: mechanisms and therapeutic potential? Clin Sci (Lond) 113:171–182.

29. **Morton GJ, Cummings DE, Baskin DG, Barsh GS, Schwartz MW**2006 Central nervous system control of food intake and body weight. Nature 443:289–295.

30. **Kievit P, Howard JK, Badman MK, Balthasar N, Coppari R, Mori H, Lee CE, Elmquist JK, Yoshimura A, Flier JS**2006 Enhanced leptin sensitivity and improved glucose homeostasis in mice lacking suppressor of cytokine signaling-3 in POMC-expressing cells. Cell Metab 4:123–132.

31. **Hill JW, Williams KW, Ye C, Luo J, Balthasar N, Coppari R, Cowley MA, Cantley LC, Lowell BB, Elmquist JK**2008 Acute effects of leptin require PI3K signaling in hypothalamic proopiomelanocortin neurons in mice. J Clin Invest 118:1796–1805. [PMCID: PMC2276395]

32. **Luo J, McMullen JR, Sobkiw CL, Zhang L, Dorfman AL, Sherwood MC, Logsdon MN, Horner JW, DePinho RA, Izumo S, Cantley LC**2005 Class IA phosphoinositide 3-kinase regulates heart size and physiological cardiac hypertrophy. Mol Cell Biol 25:9491–9502. [PMCID: PMC1265829]

33. **Elias CF, Aschkenasi C, Lee C, Kelly J, Ahima RS, Bjorbaek C, Flier JS, Saper CB, Elmquist JK**1999 Leptin differentially regulates NPY and POMC neurons projecting to the lateral hypothalamic area. Neuron 23:775–786.

34. **Kerouz NJ, Hörsch D, Pons S, Kahn CR**1997 Differential regulation of insulin receptor substrates-1 and -2 (IRS-1 and 2). J Clin Invest 100:3164–3172. [PMCID: PMC508530]

35. **Pfluger PT, Kirchner H, Günnel S, Schrott B, Perez-Tilve D, Fu S, Benoit SC, Horvath T, Joost HG, Wortley KE, Sleeman MW, Tschöp MH**2008 Simultaneous deletion of ghrelin and its receptor increases motor activity and energy expenditure. Am J Physiol Gastrointest Liver Physiol 294:G610–G618.

36. **Duplain H, Burcelin R, Sartori C, Cook S, Egli M, Lepori M, Vollenweider P, Pedrazzini T, Nicod P, Thorens B, Scherrer U**2001 Insulin resistance, hyperlipidemia, and hypertension in mice lacking endothelial nitric oxide synthase. Circulation 104:342–345.

37. **Chen D, Mauvais-Jarvis F, Bluher M, Fisher SJ, Jozsi A, Goodyear LJ, Ueki K, Kahn CR**2004 p50α/p55α phosphoinositide 3-kinase knockout mice exhibit enhanced insulin sensitivity. Mol Cell Biol 24:320–329. [PMCID: PMC303335]

38. **Mauvais-Jarvis F, Ueki K, Fruman DA, Hirshman MF, Sakamoto K, Goodyear LJ, Iannacone M, Accili D, Cantley LC, Kahn CR**2002 Reduced expression of the murine p85α subunit of phosphoinositide 3-kinase improves insulin signaling and ameliorates diabetes. J Clin Invest 109:141–149. [PMCID: PMC150818]

39. **Terauchi Y, Tsuji Y, Satoh S, Minoura H, Murakami K, Okuno A, Inukai K, Asano T, Kaburagi Y, Ueki K, Nakajima H, Hanafusa T, Matsuzawa Y, Sekihara H, Yin Y, Barrett JC, Oda H, Ishikawa T, Akanuma Y, Komuro I, Suzuki M, Yamamura K, Kodama T, Suzuki H, Yamamura K, Kodama T, Suzuki H, Koyasu S, Aizawa S, Tobe K, Fukui Y, Yazaki Y, Kadowaki T**1999 Increased insulin sensitivity and hypoglycaemia in mice lacking the p85α subunit of phosphoinositide 3-kinase. Nat Genet 21:230–235.

40. **Fruman DA, Snapper SB, Yballe CM, Davidson L, Yu JY, Alt FW, Cantley LC**1999 Impaired B cell development and proliferation in absence of phosphoinositide 3-kinase p85α. Science 283:393–397.

41. **Jacobson PB, von Geldern TW, Ohman L, Osterland M, Wang J, Zinker B, Wilcox D, Nguyen PT, Mika A, Fung S, Fey T, Goos-Nilsson A, Grynfarb M, Barkhem T, Marsh K, Beno DW, Nga-Nguyen B, Kym PR, Link JT, Tu N, Edgerton DS, Cherrington A, Efendic S, Lane BC, Opgenorth TJ**2005 Hepatic glucocorticoid receptor antagonism is sufficient to reduce elevated hepatic glucose output and improve glucose control in animal models of type 2 diabetes. J Pharmacol Exp Ther 314:191–200.

42. **Rizza RA, Mandarino LJ, Gerich JE**1982 Cortisol-induced insulin resistance in man: impaired suppression of glucose production and stimulation of glucose utilization due to a postreceptor detect of insulin action. J Clin Endocrinol Metab 54:131–138.

43. **Zinker B, Mika A, Nguyen P, Wilcox D, Ohman L, von Geldern TW, Opgenorth T, Jacobson P**2007 Liver-selective glucocorticoid receptor antagonism decreases glucose production and increases glucose disposal, ameliorating insulin resistance. Metabolism 56:380–387.

44. **Elchebly M, Payette P, Michaliszyn E, Cromlish W, Collins S, Loy AL, Normandin D, Cheng A, Himms-Hagen J, Chan CC, Ramachandran C, Gresser MJ, Tremblay ML, Kennedy BP**1999 Increased insulin sensitivity and obesity resistance in mice lacking the protein tyrosine phosphatase-1B gene. Science 283:1544–1548.

45. **Mizuno TM, Kelley KA, Pasinetti GM, Roberts JL, Mobbs CV**2003 Transgenic neuronal expression of proopiomelanocortin attenuates hyperphagic response to fasting and reverses metabolic impairments in leptin-deficient obese mice. Diabetes 52:2675–2683.

46. **Belgardt BF, Husch A, Rother E, Ernst MB, Wunderlich FT, Hampel B, Klöckener T, Alessi D, Kloppenburg P, Brüning JC**2008 PDK1 deficiency in POMC-expressing cells reveals FOXO1-dependent and -independent pathways in control of energy homeostasis and stress response. Cell Metab 7:291–301.

47. **Könner AC, Janoschek R, Plum L, Jordan SD, Rother E, Ma X, Xu C, Enriori P, Hampel B, Barsh GS, Kahn CR, Cowley MA, Ashcroft FM, Brüning JC**2007 Insulin action in AgRP-expressing neurons is required for suppression of hepatic glucose production. Cell Metab 5:438–449.

48. **Plum L, Ma X, Hampel B, Balthasar N, Coppari R, Münzberg H, Shanabrough M, Burdakov D, Rother E, Janoschek R, Alber J, Belgardt BF, Koch L, Seibler J, Schwenk F, Fekete C, Suzuki A, Mak TW, Krone W, Horvath TL, Ashcroft FM, Brüning JC**2006 Enhanced PIP3 signaling in POMC neurons causes KATP channel activation and leads to diet-sensitive obesity. J Clin Invest 116:1886–1901. [PMCID: PMC1481658]

49. **Ueki K, Yballe CM, Brachmann SM, Vicent D, Watt JM, Kahn CR, Cantley LC**2002 Increased insulin sensitivity in mice lacking p85beta subunit of phosphoinositide 3-kinase. Proc Natl Acad Sci USA 99:419–424. [PMCID: PMC117575]

50. **Gildea JJ, Herlevsen M, Harding MA, Gulding KM, Moskaluk CA, Frierson HF, Theodorescu D** 2004 PTEN can inhibit *in vitro* organotypic and *in vivo*orthotopic invasion of human bladder cancer cells even in the absence of its lipid phosphatase activity. Oncogene 23:6788–6797.

51. **Gu J, Tamura M, Pankov R, Danen EH, Takino T, Matsumoto K, Yamada KM**1999 Shc and FAK differentially regulate cell motility and directionality modulated by PTEN. J Cell Biol 146:389–403. [PMCID: PMC2156182]

52. **Patterson KI, Brummer T, O'Brien PM, Daly RJ**2009 Dual-specificity phosphatases: critical regulators with diverse cellular targets. Biochem J 418:475–489.

53. **Weng LP, Smith WM, Brown JL, Eng C**2001 PTEN inhibits insulin-stimulated MEK/MAPK activation and cell growth by blocking IRS-1 phosphorylation and IRS-1/Grb-2/Sos complex formation in a breast cancer model. Hum Mol Genet 10:605–616.

54. **Gu J, Tamura M, Yamada KM**1998 Tumor suppressor PTEN inhibits integrin- and growth factor-mediated mitogen-activated protein (MAP) kinase signaling pathways. J Cell Biol 143:1375–1383. [PMCID: PMC2133067]

55. **Asarian L, Geary N**2002 Cyclic estradiol treatment normalizes body weight and restores physiological patterns of spontaneous feeding and sexual receptivity in ovariectomized rats. Horm Behav 42:461–471.

56. **Malyala A, Kelly MJ, Rønnekleiv OK**2005 Estrogen modulation of hypothalamic neurons: activation of multiple signaling pathways and gene expression changes. Steroids 70:397–406.

57. **Wardlaw SL, Thoron L, Frantz AG**1982 Effects of sex steroids on brain β-endorphin. Brain Res 245:327–331.

58. **Chantry D, Vojtek A, Kashishian A, Holtzman DA, Wood C, Gray PW, Cooper JA, Hoekstra MF**1997 p110Δ, a novel phosphatidylinositol 3-kinase catalytic subunit that associates with p85 and is expressed predominantly in leukocytes. J Biol Chem 272:19236–19241.

59. **Hu P, Mondino A, Skolnik EY, Schlessinger J**1993 Cloning of a novel, ubiquitously expressed human phosphatidylinositol 3-kinase and identification of its binding site on p85. Mol Cell Biol 13:7677–7688. [PMCID: PMC364839]

60. **Otsu M, Hiles I, Gout I, Fry MJ, Ruiz-Larrea F, Panayotou G, Thompson A, Dhand R, Hsuan J, Totty N, et al**1991 Characterization of two 85 kDa proteins that associate with receptor tyrosine kinases, middle-T/pp60c-src complexes, and PI3-kinase. Cell 65:91–104.

61. **Knight ZA, Gonzalez B, Feldman ME, Zunder ER, Goldenberg DD, Williams O, Loewith R, Stokoe D, Balla A, Toth B, Balla T, Weiss WA, Williams RL, Shokat KM**2006 A pharmacological map of the PI3-K family defines a role for p110α in insulin signaling. Cell 125:733–747. [PMCID: PMC2946820]

62. **Jia S, Liu Z, Zhang S, Liu P, Zhang L, Lee SH, Zhang J, Signoretti S, Loda M, Roberts TM, Zhao JJ**2008 Essential roles of PI(3)K-p110β in cell growth, metabolism and tumorigenesis. Nature 454:776–779. [PMCID: PMC2750091]

Figures and Tables

Figure 1
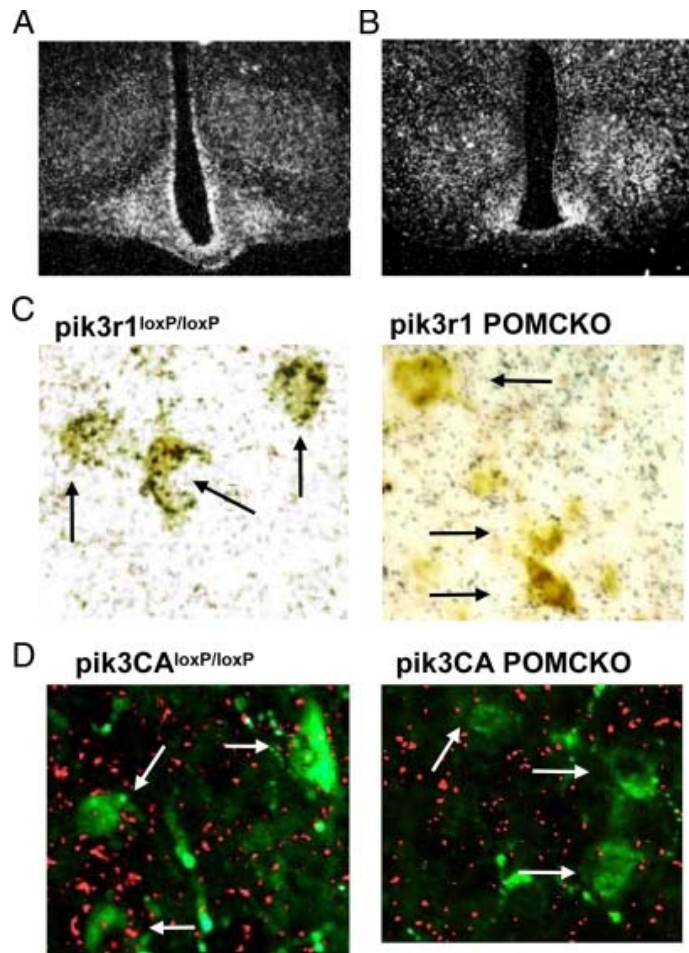
Targeted p85α or p110α deletion in POMC neurons. Photomicrographs of hypothalami from 3-month-old wild-type mice hybridized with probes for p85α (A) or p110α (B). Mice expressing Cre recombinase (Cre) under *Pomc* promoter control were mated with mice carrying loxp-flanked p85α or p110α alleles. Immunohistochemistry for β-endorphin was performed after ISHH for p85α (C) or p110α (D) in brain slices from targeted knockouts and littermate controls. *Green*, β-Endorphin immunofluorescence; *fuchsia*, p110α precipitated silver grains. *Arrows* indicate neurons in which double labeling is present (*pik3r1^{loxP/loxP}* and *pik3CA^{loxP/loxP}* mice) or absent (*pik3r1 POMCKO and pik3CA POMCKO mice). *, P* < 0.05; **, *P* < 0.01.

Figure 2
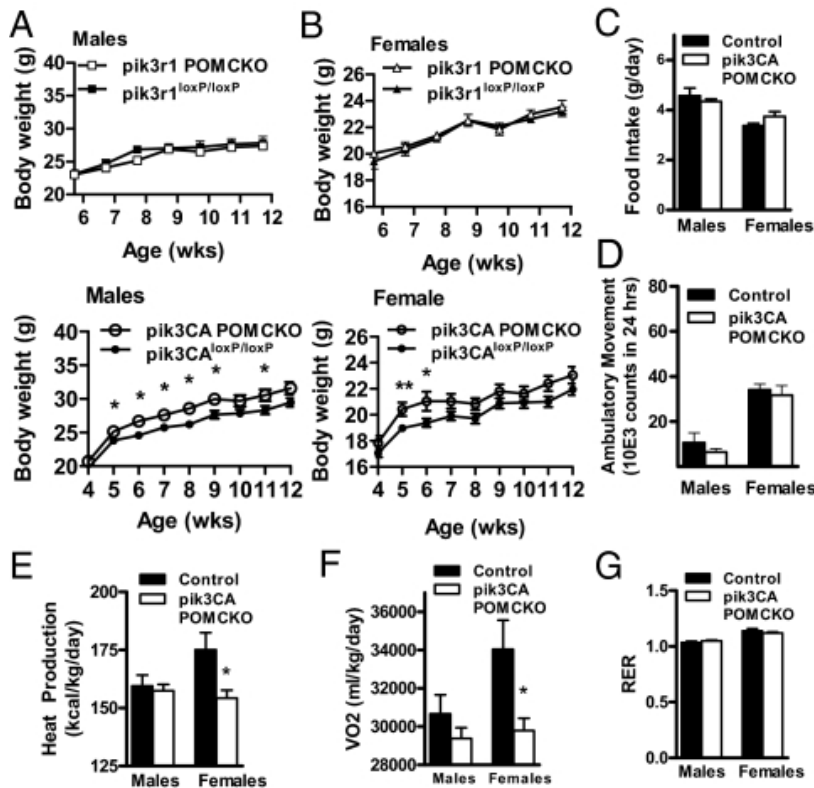
Deletion of p85α or p110α in POMC neurons impacts body weight and metabolic parameters. A, Weekly weight gain in male *pik3r1 POMCKO* mice or *pik3CA POMCKO* mice and littermate controls on normal chow ($P = 0.024$, n = 7–11). B, Weight gain in female *pik3r1 POMCKO* mice or *pik3CA POMCKO* mice and littermate controls on normal chow ($P = 0.42$, n = 7–17). Food intake (C), ambulatory movement (D), heat production (E), O_2 consumption (F), and respiratory exchange ratio (G) of 3-month-old chow-fed female *pik3r1 POMCKO* mice, *pik3CA POMCKO* mice, and their littermate controls were measured by the TSE metabolic system over a 32-h time period (n = 6–9 all groups). *, $P < 0.05$.

Figure 3
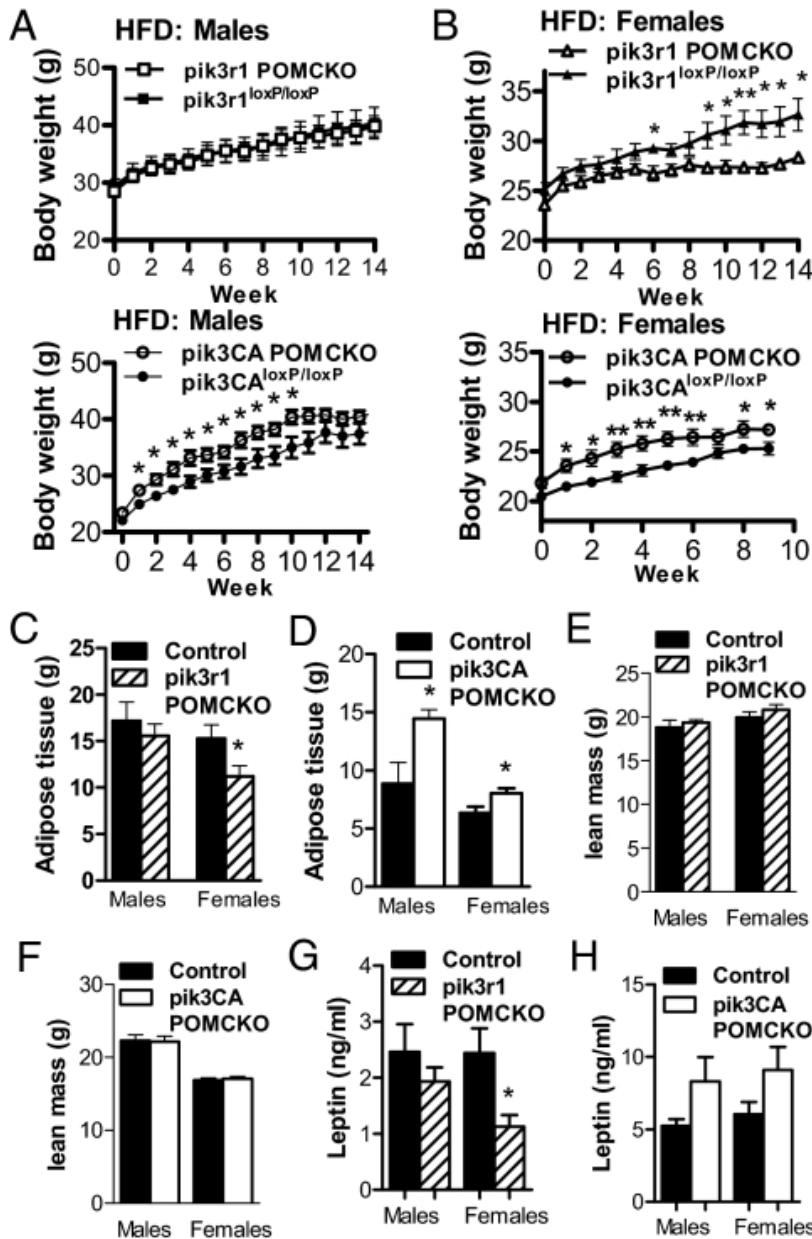
Altered body weight and adiposity in high-fat chow-fed (HFD) mice lacking p85α or p110α in POMC neurons. Weight gain in male (A) and female (B) *pik3r1 POMCKO* or *pik3CA POMCKO* mice and littermate controls were measured after introduction of high-fat chow at 3 months of age (P = 0.030 for *pik3CA POMCKO* males, P = 0.015 for *pik3r1 POMCKO* females and P = 0.008 for *pik3CA POMCKO* females; n = 7–8 male and 10–12 female cohorts). C–F, Fat and lean mass in 5-month-old *pik3r1 POMCKO*, *pik3CA POMCKO*, and littermate controls were analyzed by DEXA (*pik3r1 POMCKO* cohorts) or nuclear magnetic resonance (*pik3CA POMCKO* cohorts) (n = 6–12). G and H, Serum leptin levels were assessed by ELISA in 4-month-old *pik3r1 POMCKO, pik3CA POMCKO*, and littermate controls (n = 6–7). *, P < 0.05; **, P < 0.01.

Figure 4
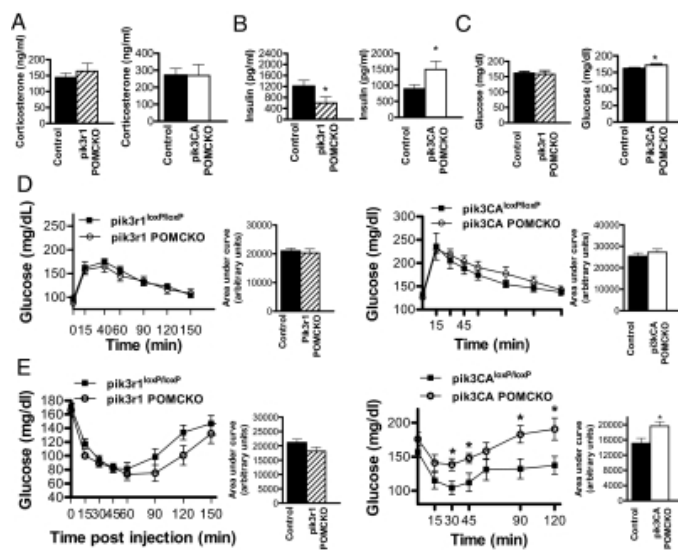
Impaired insulin responsiveness in mice lacking p110α in POMC neurons A, Corticosterone levels (nanograms per milliliter) of *pik3r1 POMCKO*, *pik3CA POMCKO*, and littermate control mice (n = 6–8), while undergoing a glucose tolerance test. Tail vein blood samples were drawn 30 min into the test. B, Serum insulin levels were measured by ELISA after removal of food for 2 h in male *pik3r1 POMCKO*, *pik3CA POMCKO*, and Cre-negative littermate controls (n = 6–10). C, Blood glucose levels were measured by glucometer after removal of food for 2 h in male *pik3r1 POMCKO*, *pik3CA POMCKO*, and littermate controls (n = 6–8). Blood glucose response curve for glucose (D) and insulin (E) tolerance tests in *pik3r1 POMCKO*, *pik3CA POMCKO*, and littermate control mice (n = 6–8) is shown. Calculated areas under the curves are displayed adjacent to each. Tolerance tests were performed on male mice with 2 g glucose/kg or 1 U of insulin/kg body weight. For all of these experiments, the mice were 3 months of age; body weight of control and experimental mice did not differ significantly. Results are expressed as mean blood glucose concentration ± SEM. *, $P < 0.05$.

Figure 5
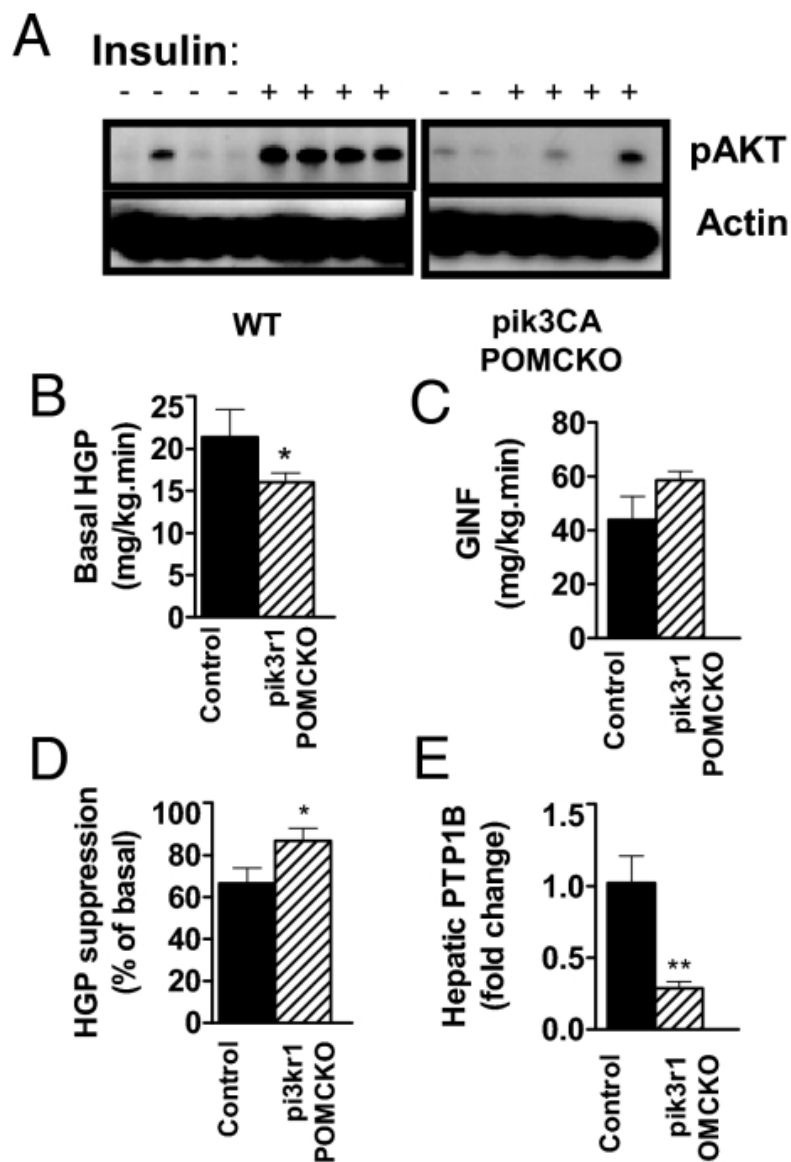
Corresponding changes in hepatic insulin sensitivity result from altered PI3K signaling in POMC neurons. A, Western blot analysis showed that phosphor-Akt (Ser-473) levels were dramatically reduced in *pik3CA POMCKO* hepatic tissue after insulin stimulation (5 U/kg ip, 10 min time point) compared with controls. Basal HGP (B) glucose infusion rate (C) and (D) suppression of HGP *in vivo* during hyperinsulinemic-euglycemic clamps in awake mice at 12–16 wk of age (*pik3r1 POMCKO* and controls, n = 8) are shown. E, PTP1B gene expression in male *pik3r1 POMCKO* and littermate controls after hyperinsulinemic-euglycemic clamp (n = 5–7). Body weights of control and experimental mice did not differ significantly. *, $P < 0.05$; **, $P < 0.01$. WT, Wild type; GINF, glucose infusion rate.